

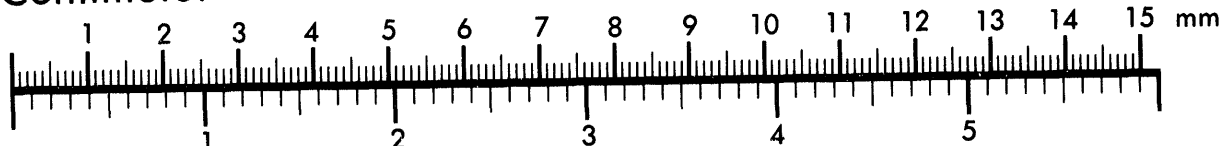


AIIM

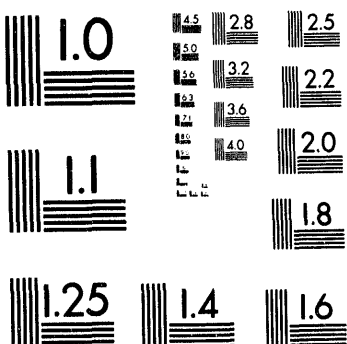
Association for Information and Image Management

1100 Wayne Avenue, Suite 1100
Silver Spring, Maryland 20910
301/587-8202

Centimeter



Inches



MANUFACTURED TO AIIM STANDARDS
BY APPLIED IMAGE, INC.

1 of 1

Conf-9405/59-3

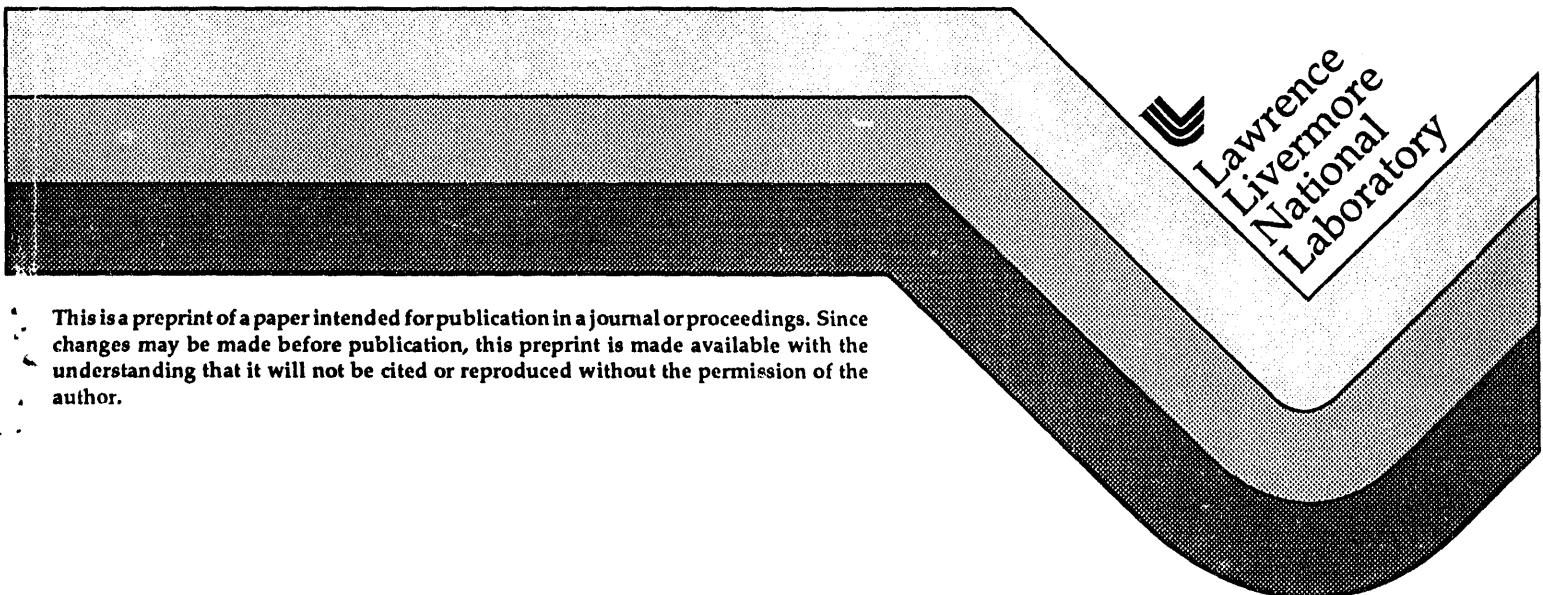
UCRL-JC-117191
PREPRINT

Subsurface Object Position and Image Correction for Standoff Ground Penetrating Radar

R. J. Kane

This paper was prepared for submittal to the
UXO Detection and Range - Remediation Conference
Golden, CO
May 17-19, 1994

May 1994



This is a preprint of a paper intended for publication in a journal or proceedings. Since changes may be made before publication, this preprint is made available with the understanding that it will not be cited or reproduced without the permission of the author.

DISTRIBUTION OF THIS DOCUMENT IS UNLIMITED

YJ

DISCLAIMER

This document was prepared as an account of work sponsored by an agency of the United States Government. Neither the United States Government nor the University of California nor any of their employees, makes any warranty, express or implied, or assumes any legal liability or responsibility for the accuracy, completeness, or usefulness of any information, apparatus, product, or process disclosed, or represents that its use would not infringe privately owned rights. Reference herein to any specific commercial products, process, or service by trade name, trademark, manufacturer, or otherwise, does not necessarily constitute or imply its endorsement, recommendation, or favoring by the United States Government or the University of California. The views and opinions of authors expressed herein do not necessarily state or reflect those of the United States Government or the University of California, and shall not be used for advertising or product endorsement purposes.

ABSTRACT

Present applications of standoff (airborne) Ground Penetrating SAR allows objects near the surface to be detected but only provides an approximation for the actual location and image. When single media models are employed the lack of correction for the phase velocity and refractive changes at the air/soil interface result in object distortions. Positional errors and image distortions comparable to the size of the object are possible. Correction is possible, if the media properties are known, by modeling the scene as a two-layer medium and accounting for the propagation effects. The propagation parameters for the lower media are estimated in the "migration" of observable responses for surface and subsurface objects. This approach allows for corrected images to subsurface objects to be produced after data collection. Surface objects will be distorted as a result of this process. The modeling process, simulations, and results with field data will be discussed.

Introduction

Ground Penetrating Radar (GPR) systems can be classified into two general categories based on employment of their antennas. In the first category, the transmitter and receiver antenna(s) are placed close to the ground. This allows the system to be designed to compensate for propagation across the air-earth interface. These systems have good depth penetrating capability but a relatively small field of view in the ground. The second category, "standoff" GPR, uses an antenna positioned some distance from the air-earth interface. This approach provides a much larger antenna footprint on the ground enabling a wider area to be viewed with the added difficulty of dealing with the air-earth interface.

The standoff GPR approach does not provide the depth of penetration capability possible with GPR systems using antennas in close proximity to the ground. The reflection/refraction process at the air-earth boundary results in time distortions and signal losses. Also, the form of data analysis employed for Synthetic Aperture Radar (SAR) imaging is generally intended for a single type of propagation media. Modeling of the interface layer as part of the data analysis to improve depth penetration is addressed in this paper. An improvement by a factor of two is significant since it would enable some applications of the standoff radar to detect objects at depths of a 1m or more benefiting Unexploded Ordnance (UXO) and hazardous waste site survey activities.

The Lawrence Livermore National Laboratory (LLNL) has assembled a standoff GPR system which uses SAR techniques to produce images of buried land mine fields. The system has allowed detection of mine-sized objects to a depth of 0.5m which satisfies some of the land mine detection needs. Extension of this penetration capability to a meter or more would make the system useful for initial survey activities of UXO ranges as well as toxic landfills. The primary

advantage is the ability to perform the survey without physically traversing the region being examined. Development of data analysis techniques are oriented toward the implementation of the LLNL hardware.

System Configuration

The LLNL standoff GPR system employs an impulse-like radar wave form and elevated antennas at heights of 10-15m above the ground. Rf energy is directed toward the ground at an angle of approximately 45 degrees and the radar system passes along a line parallel to the region under observation. Depth of penetration to 0.5m has been demonstrated with the existing hardware and data analysis.

Improvement of penetration performance is possible by incorporating a model of the air-earth interface. The simple situation is that of a two-layer propagation problem with the earth being modeled as a lossy dielectric. This discussion is limited to analysis of a two-layer, non-conductive, simple, geometry-only problem. It is sufficient to demonstrate that the effects of interest are observable.

Physical Model Development

The rf energy launched toward the ground layer is both reflected and refracted at the interface. The fractional portion of the energy coupled into the earth is propagated downward at a different angle and velocity than the incident rf energy. The portion that couples into the ground may subsequently interact with an object and be scattered back toward the receiving antenna experiencing additional perturbations along the path. Figure 1 is an illustration of this process.

The coupling of rf energy across the interface results in a perturbation which is sensitive to both depth and permittivity. These perturbations are visible in the time/range data and should be of use for improving the signal to noise ratio allowing an extension in depth performance. Time of propagation for the ray along the path in one direction is described as:

$$t_p = \frac{r_a}{c} + \frac{r_g}{c} \sqrt{\epsilon_g} \quad (eq\ 1)$$

and more explicitly for the given geometry:

$$t_p = \frac{1}{c \cos \theta_a} \frac{h}{c \cos \theta_g} + \frac{1}{c \cos \theta_g} d \sqrt{\epsilon_g} \quad (eq\ 2)$$

where "a" is for air, "g" the ground, and with the angles related through Snell's law. The problem is one of choosing appropriate values for the depth and permittivity.

The radar propagation time data acquired for an object located on the earth's surface describes a hyperbola. Data accumulated along a straight path with a two-layer media describe hyperbola-like patterns with some relatively minor variations. The difference in these patterns is what provides the information useful for estimating depth and permittivity. Since a simple geometry examination is used in this review the variations represent best discriminant possible. Incorporation of the appropriate electromagnetic coupling equations and the natural likelihood of physical variations will reduce the magnitude of the difference. There is an adequate difference however and pursuing the correction does appear warranted.

The radar time delay for a buried object can be computed as a function of permittivity or depth using the previous equation. The difference in time with respect to a reference object on the surface allows the variation to be examined. Figures 2 and 3 illustrate the computed one-way

propagation times for objects of various depths and fixed permittivity and for fixed depth with variable permittivities. The interesting aspect of these calculations is the small but apparent variation for small horizontal offset locations.

The source of the time variation is due to the angular change through the interface as the viewing position changes. The ray path length in the earth layer changes significantly for object positions close to the radar and less so as the range increases. An aspect that should be anticipated is that the propagation time difference between the buried object and the reference location becomes nearly a constant for large distances.

The figures indicate that the majority of range error occurs for horizontal travel distances of greater than about 5m. Figures 4 and 5 are expanded views for the propagation time difference over the range which is approximated by the antenna beam width. The time error values are computed by subtraction of the time delay that would be associated with a surface object at the same initial propagation time position. The data are indicative of the propagation delay produced by the earth portion of the model.

Measurement of the radar response of buried objects at position offsets to 20m requires a wide beam width antenna. Antennas were positioned at an altitude of 10m would require a full usable beam width of approximately 100 degrees. The alternative would be to sweep the antenna azimuthally at a given position to obtain the appropriate viewing angles to the target areas. The LLNL antennas are a form of wide bandwidth corner reflector and have a nominal beam width of 40-45 degrees. This constraints the usable portions of the range error graphs to the region of 0-5m. Azimuthal scanning is not employed with this hardware. The estimation of potential improvement in performance will be based on the limited antenna beam width of +/- 5m. System resolution must be small enough to enable discrimination of the depth over the 0-5m range.

SAR system slant range resolution is a function of the radar pulse bandwidth. A bandwidth approaching 1000 MHz is achieved with the LLNL pulse generator and antenna systems. Slant range resolution in this case is:

$$\Delta r_s = \frac{c}{2\beta} \quad (eq\ 3)$$

where β is the bandwidth.[1] In free space the slant range resolution is in the range of 15-20cm. Scaling this to the velocity of propagation in the ground with permittivity of 4 results in 8-10cm resolution.

The LLNL system uses an HP-54720D digitizing oscilloscope for signal acquisition which is capable of operating at 4Gs/s (250ps/s).¹ This time window corresponds to a length "cell" of 7.5cm in air and 3.8cm in soil with relative permittivity of 4. These factors, coupled with the usable antenna travel range, allow the signal to noise ratio improvement to be estimated.

The curves shown in Figure 4 illustrate that the rf energy returned from the buried object will "migrate" out of the time window predicted for an object at the surface.² The digitizer sampling time window is shown as the horizontal level added to the figure and is positioned to maximize the return signal in the shortest time delay bin. The received rf energy that falls into the next time window results in a broadening of the apparent target - a focusing problem. Compensation for depth would move this signal energy into the correct time window increasing the signal to noise ratio, sharpening focus, and allowing the depth to be estimated.

¹ "Gs/s" is Giga samples per second, "ps/s" is pico-seconds per sample.

² The time difference for two-way propagation is actually twice as large as what is plotted - The delay unique to the ground layer for one-way travel is shown.

The justification for the potential 3dB in performance improvement comes from the opportunity to recover the signal energy that falls outside of the correct time period. As the depth is increased the span over which the signal remains within a given time window versus travel is reduced. Variations due to differences in permittivity are much less pronounced in this limited region so the primary effect can be applied to a depth/range correction.

The potential for improvement is clearly illustrated by the predictable variations in the range/time error estimates. What remains at this point is the definition of reasonable techniques for exploiting these variations.

Methodology

Data collection techniques are largely unaffected by the need for altering the analysis process. Processing of the data may use a form of recursive or other recent-time block processing. Only a rudimentary post-processing approach will be discussed here.

The idealized approach for data collection would incorporate an antenna which is capable of performing an azimuthal scan as it traverses the field. This would eliminate the fixed beam width and allow data to be accumulated at a much greater angular spread. The general effect would be use of the range error curves in a region where the spread is more pronounced further increasing the potential for depth estimation. Signal attenuation resulting from the range increase is modest and can be compensated to some extent through the use of amplifiers.

Once data are collected there appear to be a number of methods for its analysis. The most straightforward approach would include analysis for each depth of interest using the full data set. This is analogous to changing the focus of a microscope. The depth of a specific object would be determined through a few trials and examination of the signal intensity. A maximum

intensity would be achieved for that depth which provided the correct parameter for propagation time data recorded. This process would be performed using every point in the data. Note that surface objects could be located by first processing the data in a "normal" manner and then observing that they defocus as the test depth is increased. This approach could be expected to provide the greatest potential for deep object or weak signal detection since it does not use a selection or threshold guideline.

Another technique for detection is the Hough transform. A threshold test could be applied to the raw data to find what might amount to the symmetry point in the data. The locus of points or time-offset appropriate for a specific depth could then be applied to the data. Summing the values along the modified curve results in focusing to a specific depth. Alternatively, the threshold test could be coupled with a gradient search algorithm to allow the shape of the time response to be determined and the associated depth estimated from its shape parameters. Other processing techniques are also available but all remain untested in this specific context. Future work includes processing of real data rather than just its discussion.

Future Plans

The geometric evaluation has been used to determine whether further analysis is appropriate. The opportunity to increase the signal to noise ratio and determine the approximate depth of an object makes further efforts worthwhile. At the present time only one data set exists which contains an object to which this concept may be applied. Preliminary evaluations include examination of this data for the features presented in this paper. Further efforts will incorporate modeling of the air-earth interface, ground conductivity, and object cross-section. The intent is the continued pursuit of the use of this type of radar for UXO, minefield, and waste pit survey activities.

Summary

A simple model of the propagation time to a buried object from a standoff GPR system indicates that there is a potential for estimating burial depth of the objects. The propagation of rf energy in the ground with a slight variation in the path length due to changes in the observation position. This results in a time delay which may provide adequate information for determining depth through examination of the signal to noise ratio for a specific location or object. Discrimination of objects at or near the surface and those at depths of 0.5-1m may be possible and the resulting increase in signal to noise ratio should also improve object detection resulting in increased depth of penetration performance.

Future work includes the potential to validate the process through analysis of data collected using the LLNL GPR system and further modeling and estimation which should include an appropriate model for the interactions at the air-earth interface.

Acknowledgments

The author wishes to acknowledge the efforts of the physicists, engineers, and technicians involved in the LLNL L-Division radar effort; Dr. David Fields, Dr. Charles Anderson, Mike Carter, F. Dean Lee, Terry Rossow, Steve Fulkerson, Paul Sargis, Bill Aimonetti, and others as well as those who were willing to discuss the concept; Dr. Harold Levie, and Dr. Michael Portnoff.

*This work was performed under the auspices of the U.S. Department of Energy by Lawrence Livermore National Laboratory under contract No. W-7405-Eng-48.

References

1. Wehner,D., 1987, *High Resolution Radar*, AERTECH House Inc.

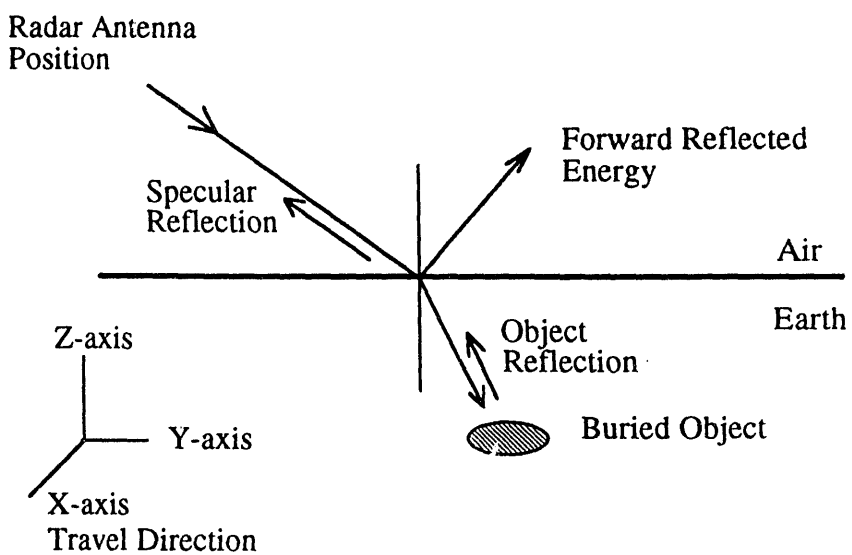


Figure 1. RF Propagation Across a Two-Layer Interface

This figure illustrates the basic two-layer propagation configuration. RF energy illuminates the air-earth boundary where some energy is reflected in the forward direction and a portion is refracted downward. Specular reflection results from surface variations. That portion of rf energy refracted into the ground may interact with an object resulting in energy being directed back toward the rf source or receiver. The aspects of interest to this work include the change in rf propagation velocity in the earth and the variation in path length as the viewing aspect is changed.

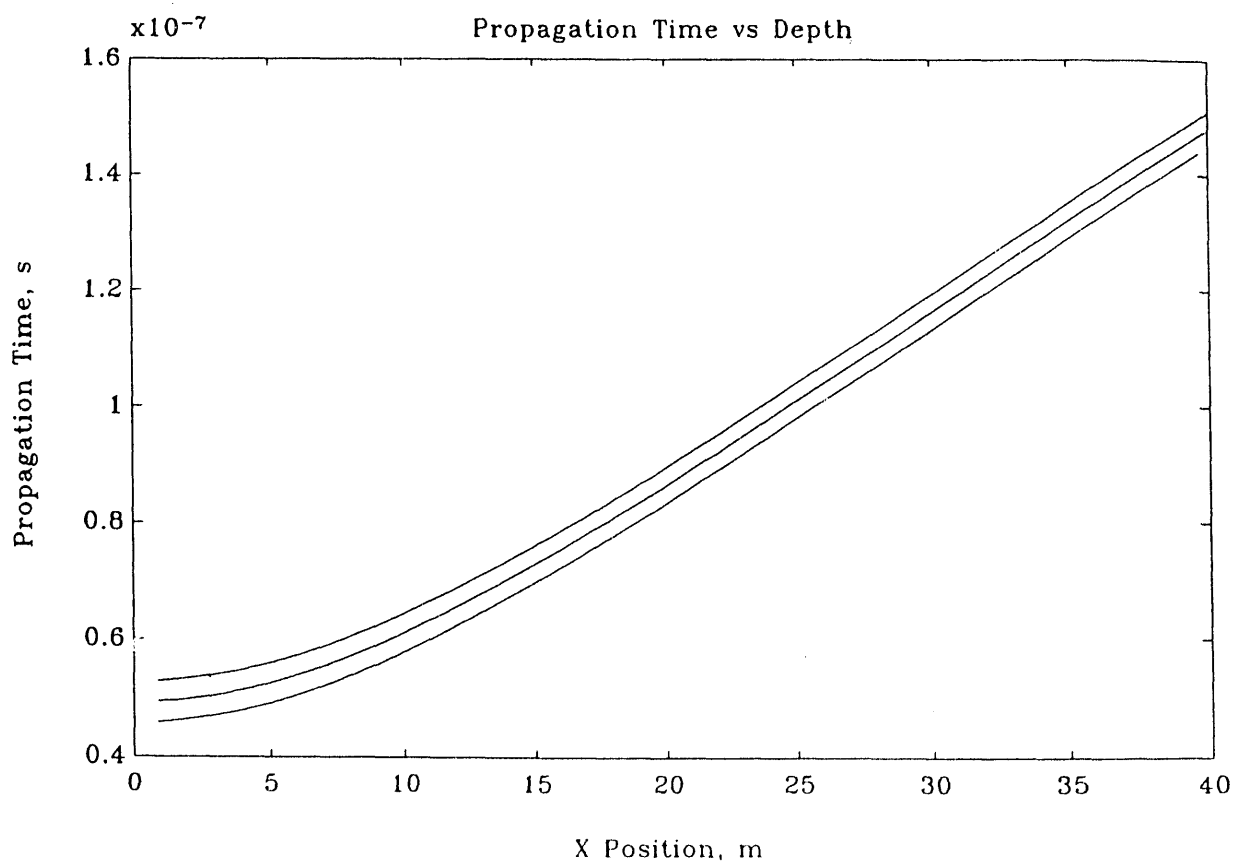


Figure 2. Propagation Time Vs Depth

The propagation time for rf from a source to an object in a fixed permittivity medium is illustrated. The three curves (left to right) correspond to depths of 2, 1.5, and 1m. The source location is at a height of 10m and constrained to move along a line in the X-axis direction.

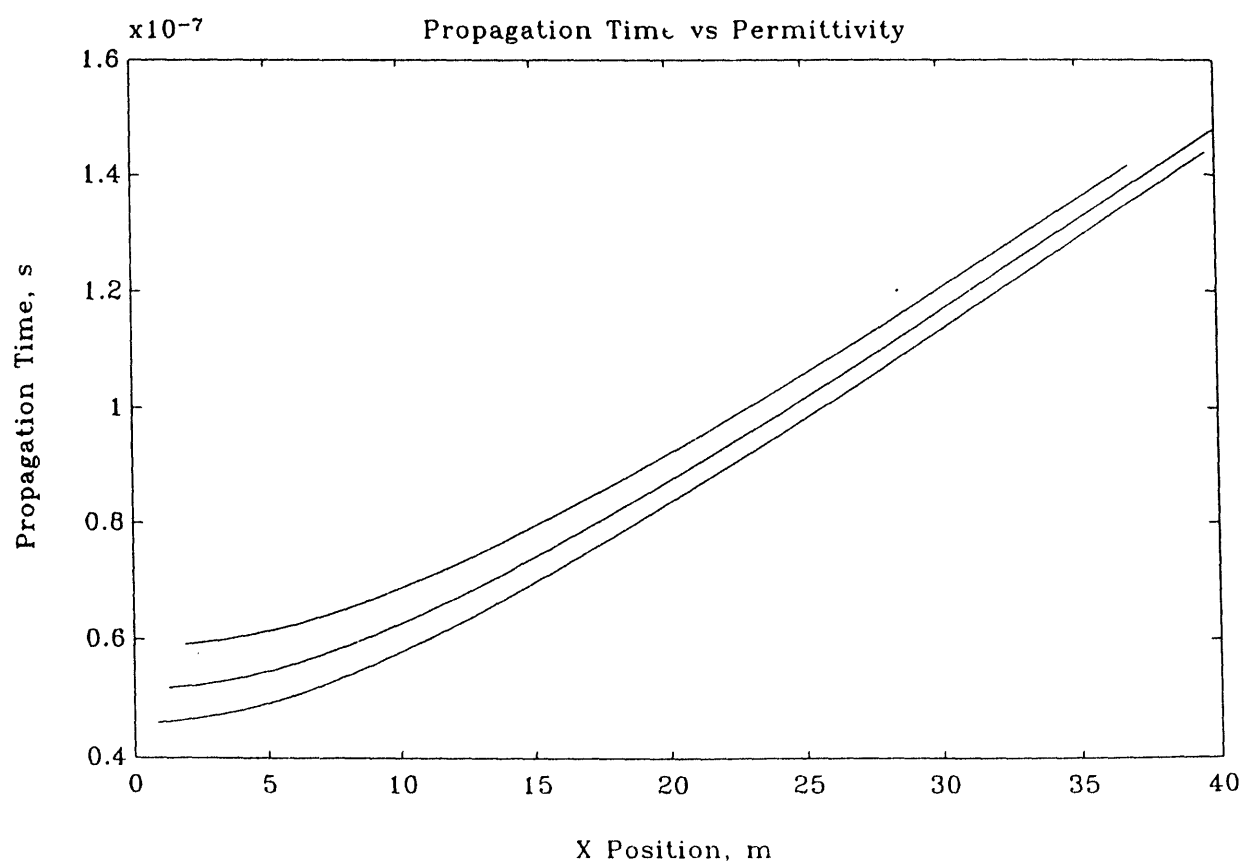


Figure 3. Propagation Time Vs Permittivity

The propagation time for an object at a depth of 1m in various permittivities is illustrated. The three curves (left to right) are for relative permittivity values corresponding to 8,6, and 4.

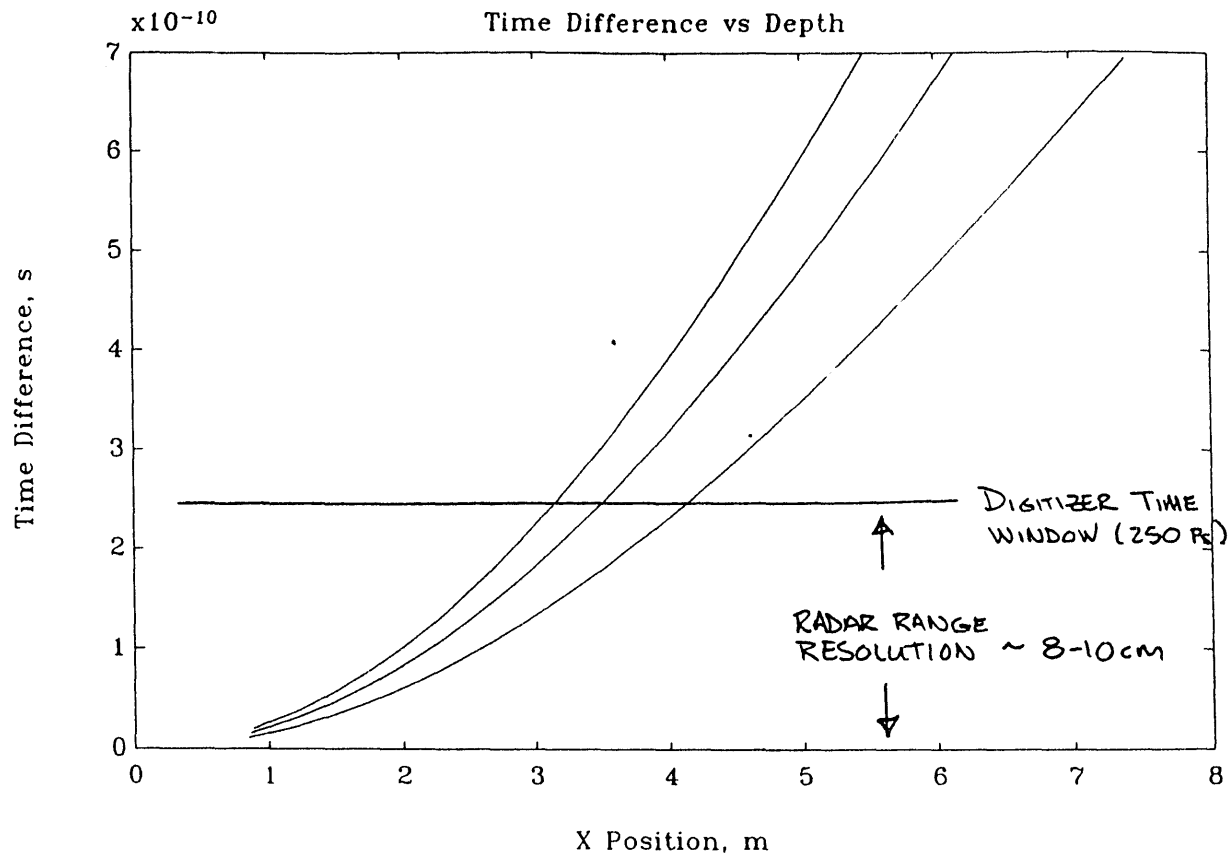


Figure 4. Propagation Time Difference Vs Depth

The difference in propagation time for a buried object referenced to a surface position is shown in this figure. As the source location moves along the X-axis the propagation path length in the earth changes and introduces the time difference illustrated. The three curves (left to right) are for object depths of 2, 1.5, and 1m. Also indicated on the figure is the sampling window of the HP-54720D digital oscilloscope and radar resolution length. Energy which lies outside of this window is defocused in the final image.

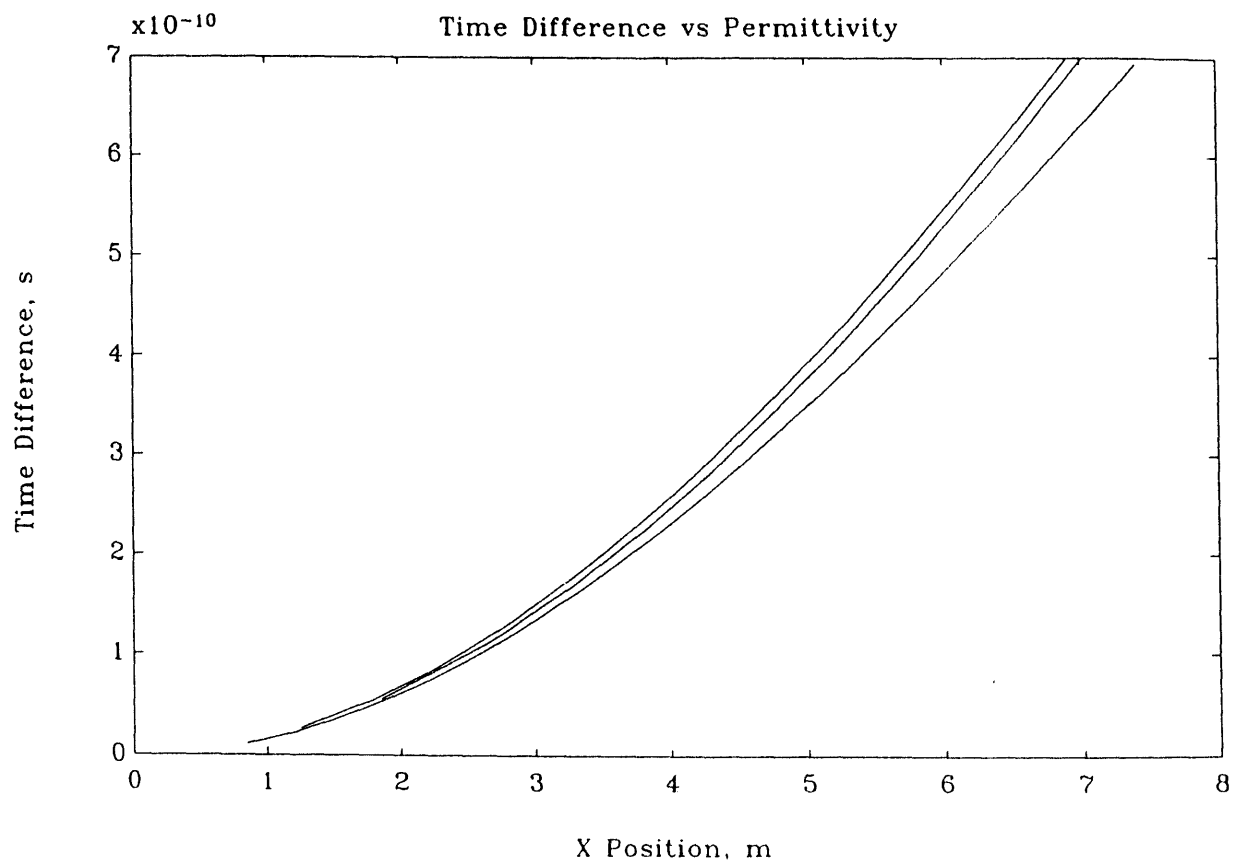


Figure 5. Propagation Time Difference Vs Permittivity

The propagation time difference of a buried object against the surface reference location is illustrated. In this figure the object depth is 1m and the earth relative permittivity (left to right) is set to values of 8,6, and 4. The time error due to permittivity changes is less significant than that for depth variation.

DATE
FILMED

8/26/94

END

